

Simulation of Heat Exchanger under Fouled Conditions

by

SIM POH KIAT

Dissertation submitted in partial fulfillment of
the requirements for the
Bachelor of Engineering (Hons)
(Chemical Engineering)

JANUARY 2009

**Universiti Teknologi PETRONAS
Bandar Seri Iskandar
31750 Tronoh
Perak Darul Ridzuan**

CERTIFICATION OF APPROVAL

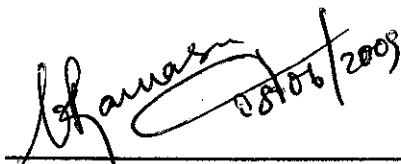
Simulation of Heat Exchanger Under Fouled Conditions

by

SIM POH KIAT

A project dissertation submitted to the
Chemical Engineering Programme
Universiti Teknologi PETRONAS
in partial fulfillment of the requirements for the
BACHELOR OF ENGINEERING (Hons)
(CHEMICAL ENGINEERING)

Approved by,



Assoc. Prof. Dr. Marappagounder Ramasamy

ABSTRACT

This dissertation reports a project on the simulation of the heat exchanger under fouled conditions. The type of fouling studied in this project is the crude oil fouling which has been categorized as a chemical reaction fouling, and is the main cause of fouling in heat exchanger. Chemical reaction fouling is a combination of heat and mass transfer, and chemical reactions. The rates of chemical reactions are difficult to predict. Fouling conditions such as fluid velocity, thermal conductivity and the film and bulk temperatures, were included in this simulation to study their effects on the performance of the heat exchanger. The threshold model will be useful to determine the threshold values for the variables in the mitigation process. The heat exchanger used in this project was a TEMA standard type AES shell and tube heat exchanger. The overall heat transfer coefficient, U was found to be $344.06 \text{ W/m}^2 \text{ K}$ with the heat transfer rate, Q of the value 4.3907 MW under clean condition. The parameters for the Ebert-Panchal model were proposed based on the types of crude oil and its blend.

ACKNOWLEDGEMENTS

First I would like to thank Assoc. Prof. Dr. Marappagounder Ramasamy, my project supervisor for his guidance in carrying out my project, till its completion.

I would also like to express my gratitude to the Chemical Engineering Department of Universiti Teknologi PETRONAS for having a final year project as one of the compulsory milestones in the degree programme. Through this project, I have the opportunity to learn a lot from my project supervisor which will be useful in my future career.

Lastly, I would like to express my gratitude to my family members for their continuous moral support that gives me the strength to carry on with my project whenever I encounter problems.

TABLE OF CONTENTS

CERTIFICATION OF APPROVAL	i
CERTIFICATION OF ORIGINALITY	ii
ABSTRACT	iii
ACKNOWLEDGEMENTS	iv
LIST OF FIGURES	vi
LIST OF TABLES	vi
ABBREVIATIONS AND NOMENCLATURES	vii
CHAPTER 1 :INTRODUCTION	1
1.1 Background Study.....	1
1.2 Problem Statement.....	4
1.3 Objectives and Scope of Study	5
CHAPTER 2: LITERATURE REVIEW	6
2.1 General Heat Transfer Design and Fouling Mechanisms Definition	6
2.2 Fouling Threshold Models	9
2.3 Pressure Drop Models.....	12
CHAPTER 3: METHODOLOGY	14
3.1 Project Methodology	14
3.2 Conventional Method Calculation	17
3.3 Bell-Delaware Method Calculation	18
CHAPTER 4: RESULTS AND DISCUSSION	31
CHAPTER 5: CONCLUSIONS AND RECOMMENDATIONS	37
REFERENCES	38
APPENDIX	41

LIST OF FIGURES

Figure 1: TEMA designation for shells and heads (BOS-HATTEN, Inc.)	15
Figure 2: Flow chart of detailed design of shell and tube heat exchanger	18
Figure 3: Gantt chart for the Final Year Project - Semester 1	29
Figure 4: Gantt chart for the Final Year Project - Semester 2	30
Figure 5: Graph of fouling resistance, R_f ($m^2\text{°C/W}$) vs time (Number of Days)	32
Figure 6: Graph of velocity (m/s) vs time (Number of Days)	33
Figure 7: Graph of fouling resistance, R_f ($m^2\text{°C/W}$) vs time (Number of Days)	34
Figure 8: Graph of fouling resistance, R_f ($m^2\text{°C/W}$) vs time (Number of Days)	35

LIST OF TABLES

Table 1: Percentage error comparison between conventional and Bell-Delaware	31
Table 2: Data on heat exchanger for clean condition	31

ABBREVIATIONS AND NOMENCLATURES

Q	the rate of heat transferred
A	the area of heat transfer surface
ΔT_{LMTD}	the log mean temperature difference
U	the overall heat transfer coefficient
h_o	“film” heat transfer coefficients on outside of the heat exchanger
h_i	“film” heat transfer coefficients on inside of the heat exchanger
l	thickness of the wall
k_m	the thermal conductivity of the metal to heat transfer
$R_{fo} + R_{fi}$	the resistance due to fouling on both side of the heat exchanger.
A_o	hot fluid surface area
A_i	cold fluid surface area
A_m	effective mean wall heat transfer area
u	the fluid velocity
d	diameter of tube for flowing fluid
μ	viscosity of the fluid
c	specific heat
μ	fluid viscosity
k	thermal conductivity
h	heat transfer coefficient
d	diameter of the tubes for flowing fluids
j	j factor
Θ_{ds}	centriangle of baffle cut
L_{bb}	Bundle-To-Shell clearance
D_{ctl}	Bundle diameter
N_b	number of baffles
Θ_{ctl}	upper centriangle of baffle cut
S_m	shell-side crossflow area
L_{tp}	tube pitch

F_w	fraction of tubes in baffle window
F_c	pure crossflow
S_b	bypass area between the shell and the tube bundle within one baffle
S_{sb}	shell-to-baffle leakage area
D_s	shell diameter
D_b	baffle diameter
S_{tb}	tube-to-baffle-hole leakage area
L_{tb}	diametral clearance between tube outside diameter and baffle hole
h_i	heat transfer coefficient for pure crossflow of an ideal tube tank.
J_c	correction factor for baffle cut and spacing
J_l	correction factor for baffle leakage effects
J_b	correction factor for the bundle bypass flow
J_s	correction factor for variable baffle spacing in the inlet and outlet sections
J_r	correction factor for adverse temperature gradient buildup in laminar flow
N_c	total number of tube rows crossed in the entire exchanger
G_s	shell side mass velocity
Re_s	shell side Reynolds Number
Pr_s	shell side Prandtl Number
j_i	ideal Colburn j factor
$(\phi_s)^n$	viscosity correction factor
$T_{s,av}$	average mean metal temperatures of shell
$T_{t,av}$	average mean metal temperatures of tube
G_t	tube side mass velocity
Re_t	tube side Reynolds Number
Pr_t	tube side Prandtl Number
A_t	tube side flow area
N_p	number of tube side passes
N_t	number of tubes

CHAPTER 1

INTRODUCTION

1.1 Background Study

Fouling is a very common phenomenon that can be observed in our daily life. By definition, fouling is a process of material deposition on to the surface. The most common occurrence of the fouling process can be observed in the heat exchangers or the heating elements in household appliances. Fouling has been categorized into several categories namely chemical reaction fouling, biological fouling, particulate fouling, crystallization fouling, corrosion fouling, and solidification fouling.

Foulant is those unwanted materials that deposited on the surface of the heat exchanger which leads to less heat transferring efficiency and the increase of pressure drop in the fouled heat exchanger. The presence of the dirt layer presents a further resistance as the thermal conductivity of a dirt layer is very much lower than the metals and the resistance is greater than both of the film resistances of the metal wall side.

With many types of fouling occurring in a single process stream, the rate is strongly dependant on local surface temperature, transport rates and shear stress. The reduction of the flow area due to the presence of the deposit, coupled with the usually rough surface presented by the foulant, increases the pressure drop through the heat exchanger. Due to the above effects, heat exchangers required additional energy to make up the energy lost due to fouling.

Heat exchangers that are handling organic fluids such as crude oil will experience a combination of a few fouling mechanisms like particulate fouling,

precipitation fouling and chemical reaction fouling. The dominant deposition mechanism that happens in the heat exchangers that heat up crude oil may be caused by the chemical reaction fouling. Chemical reaction fouling is a combination of heat and mass transfer and chemical reactions which the rates are difficult to predict.

Chemical reaction fouling for organic fluids such as crude oil can be attributed to three general classes of reactions: auto-oxidation, polymerization and thermal decomposition (Watkinson and Wilson, 1997). Heat exchanger that deals with crude oil experienced fouling originated from insoluble depositions on both the surfaces including:

- 1) Deposition of impurities found in the oil such as inorganic salts, sediments, filterable solids and corrosion products
- 2) Chemical reactions of oil constituents which are oxidative polymerization, asphaltene precipitation and coke formation.

Coke is formed by the thermal cracking of insoluble asphaltenes. Auto-oxidation of the hydrocarbons in the crude oil has been identified as the main source of unwanted deposits. Auto-oxidation fouling includes the formation of precursors which are insoluble and the transport of these precursors to the surface where they form deposits.

There are many factors that affect the fouling rate in certain equipment but the two key factors will be the film temperature and the velocity of the fluid on the wall surface. Srinivasan and Watkinson (2004) concluded that the fouling rate decreased slightly with increasing velocity and will increase with both surface and bulk temperatures.

The decisions regarding cleaning or replacement of heat exchanger tubes subject to fouling in industrial applications is based on thermo economic analysis. As the fouling of heat exchanger reduces the thermal efficiency of the equipment, an allowance needs to be introduced to compensate for the additional heat transfer resistance due to anticipated deposit which is an increase in the heat transfer area with a corresponding increase in the installed capital cost.

Tubular Exchanger Manufacturers Association, Inc. (TEMA) recommended fouling allowance are often used in the designing stage which is usually a fixed value and generally represents asymptotic value of fouling resistance, assuming the fouling process will follow an asymptotic curve. However if the fouling growth is linear with time, or according to power law or falling rate, there will be no such value. Therefore, the fouling allowance at the design stage may be treated as a critical fouling resistance, $R_{f,c}$. It is important to emphasize that incorporating additional heat-transfer area does not always solve the problem, but it may itself increase the problem of fouling, by introducing the changes, such as a decrease in the velocity as compared to the design value thus accelerating fouling growth rate.

There are a few mitigation methods known at the current stage such as:

- a) Increased tube-side velocity
- b) Using alternative baffle or tube type
- c) Accepts fouling and clean it periodically
- d) Chemical additives.

As mentioned earlier in the background study, Srinivasan and Watkinson (2004) had concluded that by increasing fluid flow velocity, the fouling rate will decrease slightly with it. With the increased fluid velocity, the insoluble precursors that are in the

flowing fluid do not have sufficient time to travel from the bulk fluid to the wall surface and be deposited there.

Most industries use the periodic cleaning method to mitigate the fouling process where there will be a certain period of time in every year that the plant operators will perform the plant shut-down and the cleaning process will take place. Instruments that are reported to have fouling will be dismantled and cleaned before installing back. This process requires a lot of time and human labour and the reinstalling process must be perfectly done or else the equipment will face exhaustion or damage due to improper installation.

There are some chemicals known as the anti-foulant which is available in the market at this moment as an alternative fouling mitigation option. Anti-foulant is to be added into the fluids that are expected to foul in the process before starting the process and are to be mixed well with the fluid. This method of fouling mitigation is quite effective but it is very costly to be used in small scale process.

1.2 Problem Statement

The performance of a heat exchanger will be severely affected by fouling. Fouling is a major problem in the chemical process industry as the problem leads to a major lost in heat energy that is being transferred in the heat exchanger. Extra heat energy is thus required to make up the lost. Besides that, fouling also leads to more severe pressure drop, and electrical energy is needed to run pumps to compensate the lost in pressure.

On the global scale, the fouling of the heat exchanger networks or the crude oil pre-heat trains had cost billions of US dollars annually. Besides that, in order to make

up the lost of the thermal energy, additional fossil fuels are needed to be burnt and this contributes to a major environmental problem.

1.3 Objectives and Scope of Study

The objectives of this project were to analyze the effects of fouling to the heat exchanger and to determine the parameters of fouling threshold model. This project also studied the effect of the known conditions that affect the degree of the fouling such as the surface temperature of the heat exchanger, the bulk temperature of the fluid, the fluid velocity and the composition of the flowing fluid. Fouling threshold models are used to determine the values of the conditions mentioned where the fouling rate is approximately at zero.

The scope of study was to determine the parameters of fouling threshold model.

CHAPTER 2

LITERATURE REVIEW

2.1 General Heat Transfer Design and Fouling Mechanisms Definition

The fouling resistance, R_f is defined as the difference in the overall heat transfer coefficient, U_f and its original value, U_o and it is shown as a mathematical expression as below:

$$R_f = \frac{1}{U_f} - \frac{1}{U_o} \quad \text{Equation 1}$$

The fundamental equation used in the design of the heat exchangers involving convective heat transfer.

$$Q = UA\Delta T_{LMTD} \quad \text{Equation 2}$$

where Q is the rate of heat transferred

A is the area of heat transfer surface

ΔT_{LMTD} is the log mean temperature difference which is the maximum driving force for heat transfer.

U is the overall heat transfer coefficient

The overall heat transfer coefficient for design is usually obtained from the equation below:

$$\frac{1}{U} = \frac{1}{h_o} + \left(\frac{1}{h_i} \times \frac{A_o}{A_i}\right) + \left(\frac{l}{k_m} \times \frac{A_o}{A_m}\right) + R_{fo} + R_{fi} \quad \text{Equation 3}$$

where h_o and h_i are the “film” heat transfer coefficients on both sides of the heat exchanger

l is the thickness of the wall (usually metal) of thermal conductivity k_m separating the two process streams 1 and 2

k_m represents the resistance of the metal to heat transfer

$R_{fo} + R_{fi}$ are the resistance due to fouling on either side of the heat exchanger.

A_o is the hot fluid surface area

A_i is the cold fluid surface area

A_m is the effective mean wall heat transfer area

Deposit on a heat transferring surface does not always develop steadily with time. Fouling scenarios such as induction period, linear fouling, falling fouling, asymptotic fouling and sawtooth fouling are often being observed and can be distinguished depending on the nature of the system and the local thermo hydraulic conditions on the surface. The fouling scenarios will be further discussed in details below.

Induction period is where a near zero fouling rate is observed when the surface is new or very clean. After this induction period, the fouling rate increases with respect to time.

Linear fouling has a fouling layer that is too tenacious to shear off at economic design velocities. The fouling layer continues to build following a roughly linear function of time. In this fouling mechanism, the rate of fouling over time is dependent on velocity. At low velocity, fouling is controlled by mass diffusion to the surface. Increasing the velocity increases the mass diffusion thus leading to increasing of the fouling rate. At high velocity, fouling is controlled by deposit shearing, residence time, and decreases with increasing velocity. This mechanism is strongly dependant on surface temperature. (Epstein 1988).

Falling rate fouling is a steadily decreasing difference between deposition flux and removal flux in which the difference approaches zero only as R_f approaches infinity, which will result in a non-asymptotic falling rate fouling curve (Epstein 1988). This

situation commonly occurs where deposit removal is negligible, as in scaling by single uncontaminated salts or in mono-dispersed colloidal particle deposition from an isothermal laminar flow field, and where the deposition flux is subjected to an auto-retardation mechanism. Some auto-retardation mechanisms include:

- a) Decrease in oxygen diffusion rate in corrosion fouling as the deposit thickens.
- b) The effect of deposit blockage in increasing the scouring velocity and thereby suppressing attachment.
- c) A progressive change in surface charge due to deposition of oppositely charged colloidal particles.
- d) An ever-weakening wall catalysis of chemical reaction fouling as the deposit builds up on the wall.
- e) A decrease of deposit-fluid interface temperature, T_s with time.

Asymptotic fouling reaches a maximum fouling resistance after a certain period of run time. Fluid velocity imparts shear stress at the fouling layer that removes some of the deposit. As the fouling layer thickens, flow area is reduced and velocity increases which leads to increasing of removal rate. The asymptotic limit is reached when the rate of removal equals the rate of deposition. The thickness of final asymptotic fouling layer is found to be inversely proportional to the original velocity.

The occurrence of sawtooth fouling mode under conditions of steady flow, fluid temperature and concentration implies periodic shedding of deposit due to periodic weakening of the deposit to a value of deposit strength (ϕ) below some critical value. Such weakening could be caused by changes in crystal structure, chemical degradation, developing thermal stresses or slow poisoning of micro-organisms in a biofilm. The critical value of ϕ would be such that the smaller of the adhesive or cohesive force of the deposit is just exceeded by the hydrodynamic forces tending to disrupt the deposit.

The persistence of an underlying deposit on the tube side while the rest of the deposit is periodically shed could be caused by the co-existence of two different types of fouling and the respectively different deposits and periodic removal over an underlying developing corrosion deposit. Periodic removal could also be caused by accidental disturbances (hydrodynamic or thermal) of particulate deposits partially bound to a metal wall where the cessation of crevice corrosion as the tube wall becomes uniformly covered with deposit, rather than continuous deposit removal (Epstein and Norman 1988).

2.2 Fouling Threshold Models

Fouling models must include parameters such as the rates of the processes that lead to deposition, the temperature distribution and the deposit thickness process and the effect of flow on deposition and re-entrainment.

There are a few models that have been used in determining the threshold fouling value. Threshold of fouling is the value where the fouling rate would be close to zero. Among all the numerical models known, Ebert and Panchal (1995) outlined a numerical model using the fouling data obtained from pilot plant and refinery side-stream monitoring tests where the rate of fouling is presented as a competition between deposition and suppression terms, shown as below:

$$\begin{aligned} \frac{dR_f}{dt} &= \textit{deposition} - \textit{suppression} \\ &= A_I Re^{-\beta} \exp\left(\frac{-E_I}{RT_f}\right) - C_I \tau_w \end{aligned} \quad \text{Equation 4}$$

and regression yielded the parameter set $\{A_I = 30.2 \times 10^6 \text{ K m}^2/\text{kWh}; \beta = 0.88, E_I = 68 \text{ kJ/mol and } C_I = 1.45 \times 10^{-4} \text{ m}^2 \cdot \text{Km}^2/\text{kW} \cdot \text{Pa} \cdot \text{h}\}$. The model was published based on an analysis of the (high temperature) furnace tube-side coking data.

The film temperature, T_f is defined as:

$$T_f = \frac{T_{wall} + T_t}{2} \quad \text{Equation 5}$$

where T_t is the bulk temperature of the fluid in tubes. The wall shear stress τ_w is linked to bulk velocity through the friction factor:

$$\tau_w = \frac{1}{2} \rho v^2 f \quad \text{with} \quad f = \frac{0.0791}{Re^{1/4}} \quad \text{Equation 6}$$

In the intervening ten years the basic formulation of the model has been revised into several variants. The consideration of the data sets obtained from both (well defined) pilot plant tests and monitoring of plant exchangers give the revised form of Equation 1 as

$$\frac{dR_f}{dt} = A_{II} Re^{-0.66} Pr^{-0.33} \exp\left(\frac{-E_{II}}{RT_f}\right) - C_{II} \tau_w \quad \text{Equation 7}$$

where the fluid flow and thermal properties are needed for the use of Prandtl Number and a fixed power on the Reynolds Number.

The Ebert-Panchal model cannot be directly used for the modelling and prediction of fouling within the shells as it assumes that the suppression mechanism is controlled by wall friction, which cannot be estimated from shell-side pressure drop as this includes a significant contribution from drag.

One approach is to apply the heat and mass transfer analogy and thereby employ the shell-side heat transfer coefficient as a measure of the wall friction and shear stress. Polley *et al.* (2002) employed a deposition term with an explicit dependence on the deposit or wall surface temperature T_s rather than film temperature T_f , and a mass transfer related suppression term:

$$\frac{dR_f}{dt} = A_{III} Re^{-0.8} Pr^{-0.33} \exp\left(\frac{-E_{III}}{RT_s}\right) - C_{III} Re^{0.8} \quad \text{Equation 8}$$

where $A_{III} = 1000000 \text{ m}^2 \text{ K W}^{-1} \text{ h}^{-1}$

$$C_{III} = 1.5 \times 10^{-9} \text{ m}^2 \text{ K W}^{-1} \text{ h}^{-1}$$

$$E_{III} = 48 \text{ kJ/mol}$$

The parameters were derived by Polley *et al.* (2002) fit in the fouling threshold data reported by Knudsen *et al.* (1999).

In Equation 8, the model assumes that the velocity dependency of fouling is linked to transport phenomena and this can be extended to cover shell-side flows and the use of tube inserts. The Chilton-Coburn j-factor for heat transfer inside tubes under turbulent flow conditions is:

$$j_h = \frac{Nu}{Pr^{0.33}} = 0.027 Re^{0.8} \quad \text{Equation 9}$$

Yeap *et al.* (2004) compared different forms of the right-hand-side (RHS) terms for a larger data set than Polley *et al.* (2002) and found best agreement with a deposition term based on the Epstein model for tube-side chemical reaction fouling with u as the tube-side mean velocity.

$$\frac{dR_f}{dt} = \frac{A_{IV} C_f u T_s^{2/3} \rho^{2/3} \mu^{-4/3}}{1 + B_{IV} u^3 C_f^2 \rho^{5/3} \mu^{-7/3} T_s^{2/3} \exp(E_{IV}/RT_s)} - C_{IV} u^{0.8} \quad \text{Equation 10}$$

In the work of Jafari Nasr and Majidi Givi (2005), they had proposed a new model as shown below. The proposed model has better prediction on fouling than the Polley *et al.* model.

$$\frac{dR_f}{dt} = \alpha Re^\beta \exp\left(\frac{-E}{RT_f}\right) - \gamma Re^{0.4} \quad \text{Equation 11}$$

and the constants used in the evaluation for Australian light crude oil are:

$$\alpha = 10.98 \text{ m}^2 \text{ K/kJ}$$

$$\beta = -1.547$$

$$\gamma = 0.96 \times 10^{-10} \text{ m}^2 \text{ K/kJ}$$

$$E = 22.618 \text{ kJ/mol}$$

2.3 Pressure Drop Models

Fouling affects pressure drop by three ways: constriction of flow area due to growth of deposit layers, increased roughness of the surface, and tube blockages that results in increased flow velocities in other tubes, hence resulted in greater pressure drop.

Yeap *et al.* (2003) showed that the overall heat transfer coefficient, U , for the constant mass flow rate scenarios, can be calculated from:

$$\frac{1}{U} = R_{ext} + \frac{r_l}{\lambda_f} \ln \left(\frac{r_l}{r_i} \right) + \frac{1}{h_l} \left(\frac{r_i}{r_l} \right) \left(\frac{C_{f,l}}{C_{f,i}} \right) \quad \text{Equation 12}$$

which can be expressed as a dimensionless fouling Biot Number $Bi_f \equiv R_f \times h_l$

$$Bi_f = -Y \ln \left(1 - \frac{\delta}{r_l} \right) + \left[\left(\frac{C_{f,l}}{C_{f,i}} \right) \left(1 - \frac{\delta}{r_l} \right) - 1 \right] \quad \text{Equation 13}$$

where $Y \equiv r_l h_l / \lambda_f$; r_l is the clean tube radius

h_l = clean tube-side heat transfer coefficient

λ_f = foulant thermal conductivity

Y is the ratio of convective and conductive resistance hence it varies strongly with the properties of the deposit.

Equation 14 indicates that as the roughness of the fouling layer increases, Bi_f decreases due to the enhanced heat transfer. In the following pressure drop model, fouling is assumed to be present only on the tube-side. The first model is due to the duct reduction effect where the friction factor is assumed to be constant:

$$\Delta P^* \equiv \frac{\Delta P}{\Delta P_1} = \left(1 - \frac{Bi_f}{Y} \right)^{-5} \quad \text{Equation 14}$$

The second pressure drop model is due to the effect of roughness as the roughness of the fouling layer will increase as deposit accumulates on the tube surface and the model is shown as below:

$$\Delta P^* \equiv \frac{\Delta P}{\Delta P_1} = \frac{C_{f,i}}{C_{f,tube}} \left(1 - \frac{Bi_f}{Y}\right)^{-5} \quad \text{Equation 15}$$

The third pressure drop model is caused by the tube blockage which leads to the tubes to be out of service, resulting in loss of heat transfer area. In the constant throughput scenario, the velocity in the remaining tubes would increase, partially compensating for the loss of heat transfer area. The form of the model for constant throughput is

$$P^* = (1 + Bi_{f,U})^{3.15} \quad \text{Equation 16}$$

All the three pressure drop models discussed earlier rely heavily on the assumed deposit distributions within the heat exchanger tubes. The second major assumption in these three models is that the foulant thermal conductivity is to have uniform values, *i.e.* zero or rapid ageing.

CHAPTER 3

METHODOLOGY

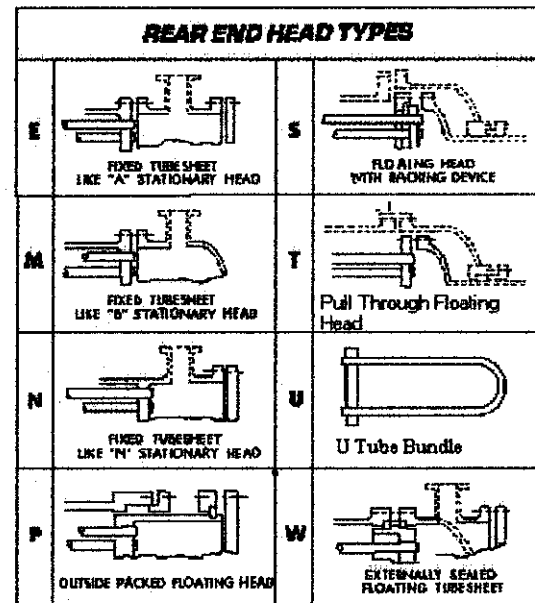
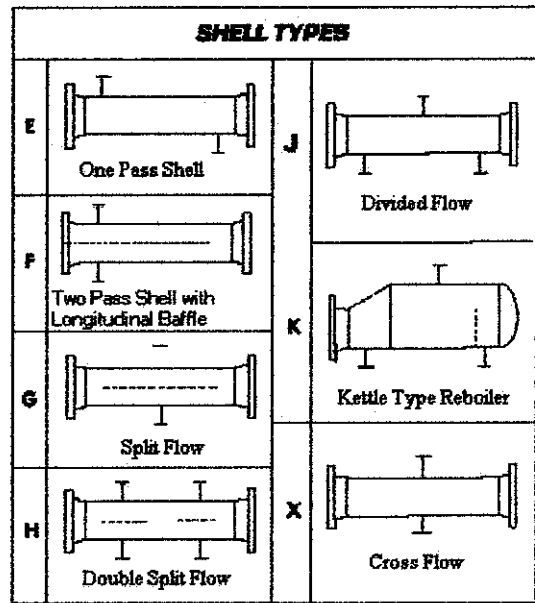
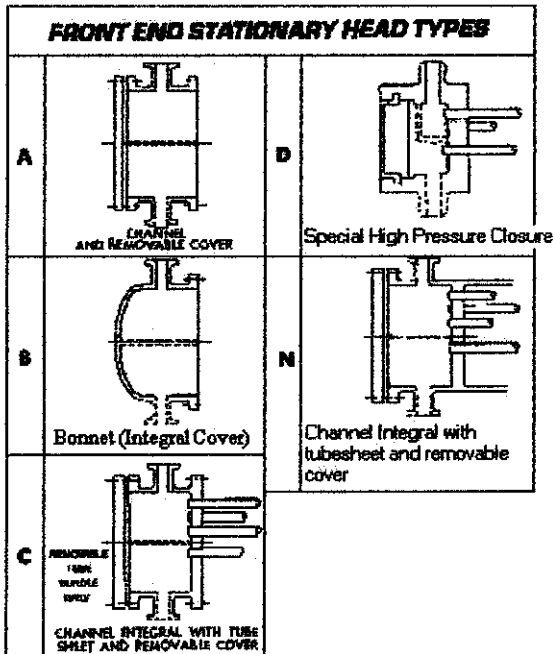
3.1 Project Methodology

This project studied the heat exchanger for crude distillation unit. The heat exchanger was constructed based on the TEMA type of AES. The configuration AES is defined as having the A type front head, E type shell design, and S type rear head. The E shell is the most common due to its cost, simplicity and ease of manufacturing. It has only one shell pass with the shell-side fluid entry and exit nozzles attached at the two opposite ends of the shell. The tube side may have a single pass or multiple passes and the tubes are supported by transverse baffles. This shell configuration is the most common for single-phase shell fluid applications.

For a heat exchanger dealing with fluids that will foul, a head or cover plate that can be easily removed is an obvious choice and this head will be connected on the sides and not on the ends of removable heads. Typical open-end heads used for this purpose are called channels and they are fitted with easily removable cover plates so that the tubes can be cleaned without disturbing the piping. The A type front head is defined based on TEMA standards as channel with removable cover while S type rear head is floating head with backing device. Further descriptions of the TEMA standard for shell-and-tube heat exchanger design are shown in Figure 1 below.

STANDARD TEMA NOMENCLATURE

TEMA (Tubular Exchangers Manufacturers Assoc.) has devised a standard nomenclature to briefly describe heat exchangers. This chart explains the 3 letter designation TEMA heat exchangers have and is a great tool for quick reference. All Bos-Hatten heat exchangers are designed to TEMA standards.



Sales Offices
BOS-HATTEN
227 Thorn Avenue
Buffalo, NY 14127
Phone: 716-662-7030 • Fax: 716-662-6548
E-mail: info@bh.nitram.com
Visit our web site www.nitram.com/boshatten

Figure 1: TEMA designations for shells and heads (BOS-HATTEN, Inc.)

In this project, the effects on the fouling rate from the different crude were studied. The crude properties are as shown in Appendix 1.

A simulation of the heat exchanger under the fouled conditions given by the project requirement was carried out. Analysis of the data obtained through the simulation was done once all the simulation processes had been completed. The simulation could be conducted using several models proposed by previous researchers that have presented their findings in this area, as an example the Ebert and Panchal model (Equation 4) was used in the project.

Before starting of the simulation process using Microsoft Excel and Matlab, some of the important design data need to be collected such as:

- a) Fluid velocities at both sides
- b) Inlet and outlet conditions of both working fluids
- c) Overall heat transfer coefficient of the heat exchanger

The overall heat transfer coefficient of the clean condition can be calculated from the data obtained either by using the conventional method or the Bell-Delaware method.

3.2 Conventional Method Calculation

For calculating the heat transfer coefficient for both sides of the heat exchanger, the data required are the fluid viscosities, the fluid velocities at both sides, the diameters of the tubes for flowing fluid, the specific heats and the thermal conductivities.

Using these data, the necessary parameters can be computed using the following equations:

$$\text{Reynolds Number, } Re = \frac{ud}{\mu} \quad \text{Equation 17}$$

where u is the fluid velocity

d is the diameter of tube for flowing fluid

μ is the viscosity of the fluid

$$\text{Prandtl Number, } Pr = \frac{c\mu}{k} \quad \text{Equation 18}$$

where c is the specific heat

μ is the fluid viscosity

k is the thermal conductivity

$$\text{Nusselt's Number, } Nu = \frac{hd}{k} = jRe^{0.8}Pr^{(0.33)} \quad \text{Equation 19}$$

where h is the heat transfer coefficient

d is the diameter of the tubes for flowing fluids

k is the thermal conductivity

j is the j factor

3.3 Bell-Delaware Method Calculation

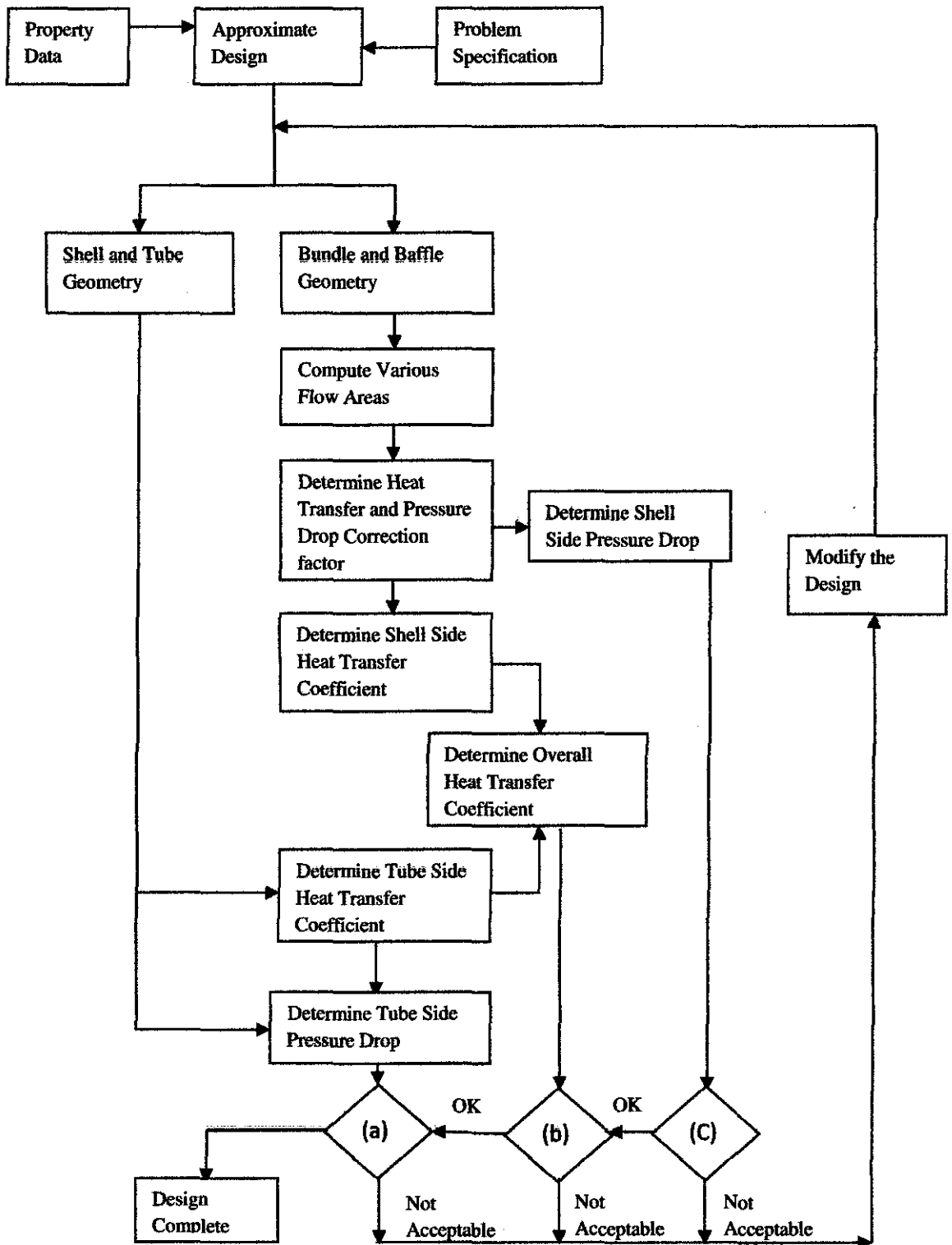


Figure 2: Flow chart of detailed design of shell and tube heat exchanger. (a) $\Delta P_t \leq$ allowed pressure drop; (b) compare area required with area available for heat transfer; and (c) $\Delta P_s \leq$ allowed pressure drop. (Kuppan, 2000).

The Bell-Delaware method assumes that the flow rate and the inlet and the outlet temperatures of the shell side fluid are specified and that the density, viscosity, thermal conductivity and specific heat of the shell side fluid are known. Other data that are required will be the outside diameter of the tube (d), the tube layout pattern (Θ_{tp}), shell inside diameter (D_s), outer tube limit diameter of the tube bank (D_{otl}), effective tube length (L_{ti}), baffle cut (B_c) as a percent of D_s , central baffle spacing (L_{bc}) and the number of sealing strips per side (N_{ss}).

From this set of geometrical parameters, all remaining geometrical parameters pertaining to the shell side can be calculated or estimated by methods given here, assuming that the standards of TEMA are met with respect to various shell side constructional details. The calculation of various geometrical parameters is known as auxiliary calculations in the Bell-Delaware method.

Shell Side Parameters

Bundle-To-Shell clearance, L_{bb} . A suitable tube bundle is selected based on the user's requirement, and the bundle-to-shell clearance is calculated from the following equations:

$$L_{bb} = D_s - D_{otl} \quad \text{Equation 20}$$

Bundle diameter (D_{ctl}) which can be computed from the equation:

$$\begin{aligned} D_{otl} &= D_s - L_{bb} \\ &= D_{ctl} + d \end{aligned} \quad \text{Equation 21}$$

The number of baffles (N_b) is required for calculation of the total number of cross passes and window turnarounds and is expressed as:

$$N_b = \frac{L_{ti}}{L_{bc}} - 1 \quad \text{Equation 22}$$

Auxiliary Calculations: Step-by-Step Procedures

Step 1: Sequential baffle window calculations

Calculate the centriangle of baffle cut (Θ_{ds}) and upper centriangle of baffle cut (Θ_{ctl}). The centriangle of baffle cut (Θ_{ds}) is the angle subtended at the centre by the intersection of the baffle cut and the inner shell wall and it is given by

$$\theta_{ds} = 2 \cos^{-1}\left(1 - \frac{2B_c}{100}\right) \quad \text{Equation 23}$$

The upper centriangle of baffle cut (Θ_{ctl}) is the angle subtended at the centre by the intersection of the baffle cut and the tube bundle diameter which is defined as:

$$\theta_{ctl} = 2 \cos^{-1}\left[\frac{D_s}{D_{ctl}}\left(1 - \frac{2B_c}{100}\right)\right] \quad \text{Equation 24}$$

Step 2: Shell-side crossflow area

The shell-side crossflow area, S_m is given by:

$$S_m = L_{bc} \left[L_{bb} + \frac{D_{ctl}}{L_{tp,eff}} (L_{tp} - d) \right] \quad \text{Equation 25}$$

where $L_{tp,eff} = L_{tp}$ for 30° and 90° layouts

= 0.707 L_{tp} for 45° staggered layout

L_{tp} = tube pitch

Step 3: Baffle window flow areas

Calculate the fraction of tubes in baffle window (F_w) and in pure crossflow (F_c) that is between the baffle cut tips.

$$F_c = 1 - 2F_w \quad \text{Equation 26}$$

$$F_w = \frac{\theta_{ctl}}{2\pi} - \frac{\sin \theta_{ctl}}{2\pi} \quad \text{Equation 27}$$

Step 4: Bundle-to-shell bypass area parameters (S_b and F_{sbp})

The bypass area between the shell and the tube bundle within one baffle (S_b) is given by:

$$S_b = L_{bc}(D_s - D_{otl} + L_{pl}) \quad \text{Equation 28}$$

where L_{pl} expresses the effect of the tube lane partition bypass width (between tube walls) as follows: L_{pl} is 0 for all standard calculations; L_{pl} is half the dimension of the tube lane partition L_p . For estimation purposes, assume that $L_p = d$.

For calculations of the correction factors J_1 and R_1 , the ratio of the bypass area (S_b) to the overall crossflow area (S_m) designated as F_{sbp} is calculated from the expression:

$$F_{sbp} = \frac{S_b}{S_m} \quad \text{Equation 29}$$

Step 5: Shell-to-baffle leakage area for one baffle (S_{sb})

The shell-to-baffle leakage area (S_{sb}) is a factor for calculating baffle leakage effect parameters J_1 and R_1 . The diametral clearance between the shell diameter D_s and the baffle diameter D_b is designated as L_{sb} and given by:

$$L_{sb} = \left(\frac{3.1 + 0.004D_s}{2 \times 1000} \right) \quad \text{Equation 30}$$

The shell-to-baffle leakage area within the circle segment occupied by the baffle is calculated as:

$$S_{sb} = \pi D_s \frac{L_{sb}}{2} \left(\frac{2\pi - \theta_{ds}}{2\pi} \right) \quad \text{Equation 31}$$

Step 6: Tube-to-baffle-hole leakage area for one baffle (S_{tb})

The tube-to-baffle-hole leakage area for one baffle (S_{tb}) is required for calculating the correction factors J_1 and R_1 . The total tube-to-baffle-hole leakage area is given by

$$S_{tb} = \frac{\pi}{4} [(d + L_{tb})^2 - d^2] N_t (1 - F_w) \quad \text{Equation 32}$$

where L_{tb} is diametral clearance between tube outside diameter and baffle hole. TEMA standards specify recommended this clearance as a function of tube diameter and baffle spacing which value is either 0.8 or 0.4.

Shell-Side Heat Transfer Correction Factors

In Bell-Delaware method, the flow fraction for each stream is computed from the corresponding flow areas and flow resistances. The heat transfer coefficient for ideal crossflow is then modified for the presence of each stream through correction factors. The shell side heat transfer coefficient is defined as:

$$h_s = h_i J_c J_1 J_b J_s J_r \quad \text{Equation 33}$$

where h_i is the heat transfer coefficient for pure crossflow of an ideal tube tank. The correction factors in Equation 33 are as follows:

J_c is the correction factor for baffle cut and spacing. This correction factor is used to express the effects of the baffle window on the shell side ideal heat transfer coefficient h_i , which is based on crossflow.

J_1 is the correction factor for baffle leakage effects, including both shell-to-baffle and tube-to-baffle leakage.

J_b is the correction factor for the bundle bypass flow

J_s is the correction factor for variable baffle spacing in the inlet and outlet sections

J_r is the correction factor for adverse temperature gradient buildup in laminar flow

Step 7: Segmental baffle window correction factor (J_c)

For the baffle cut range of 15% to 45%, J_c is expressed as:

$$J_c = 0.55 + 0.72F_c \quad \text{Equation 34}$$

Step 8: Correction factors for baffle leakage effects for heat transfer (J_l)

The correction factor J_l penalizes the design if the baffles are put too close together, leading to an excessive fraction of the flow being in the leakage streams compared to the crossflow stream.

$$J_l = 0.44(1 - r_s) + [1 - 0.44(1 - r_s)]e^{-2.2r_{lm}} \quad \text{Equation 35}$$

$$\text{where } r_s = \frac{S_{sb}}{S_{sb} + S_{tb}} \quad \text{Equation 36}$$

$$r_{lm} = \frac{S_{sb} + S_{tb}}{S_m} \quad \text{Equation 37}$$

Step 9: Correction factors for bundle bypass effects for heat transfer (J_b)

$$J_b = \exp\left\{-C_{bb}F_{sbp}\left[1 - (2r_s)^{\frac{1}{3}}\right]\right\} \quad \text{Equation 38}$$

where $C_{bb} = 1.25$ for laminar flow ($Re \leq 100$) with the limit of $J_b = 1$ at $r_s \geq 0.5$
 $= 1.35$ for turbulent and transition flow ($Re > 100$)

For a relatively small clearance between the shell and the tube bundle, J_b is about 0.9; for a much larger clearance required by pull through floating head construction, it is about 0.7. J_b can be improved by using sealing strips.

Step 10: Heat transfer correction factor for adverse temperature gradient in laminar flow (J_r)

J_r applies only if the shell side Reynolds Number is less than 100 and is fully effective only in deep laminar flow characterized by Re_s less than 20.

$$\text{For } Re_s < 20, J_r = \frac{1.51}{N_c^{0.18}} \quad \text{Equation 39}$$

$$\text{For } 20 \leq Re_s \leq 100, J_r = \frac{1.51}{N_c^{0.18}} + \left(\frac{20 - Re_s}{80}\right)\left(\frac{1.51}{N_c^{0.18}} - 1\right) \quad \text{Equation 40}$$

where N_c is the total number of tube rows crossed in the entire exchanger which is

$$N_c = (N_{tcc} + N_{tcw})(N_b + 1) \quad \text{Equation 41}$$

With the limit of $J_r=0.4$ for $Re_s \leq 100$ and $J_r=1$ for $Re_s > 100$.

Step 11: Heat transfer correction for unequal baffle spacing at inlet and/or outlet

(J_s)

$$J_s = \frac{(N_b-1)+(L_i^*)^{1-n}+(L_o^*)^{1-n}}{(N_b-1)+(L_i^*-1)+(L_o^*-1)} \quad \text{Equation 42}$$

$$\text{where } L_i^* = \frac{L_{bi}}{L_{bc}} \quad \text{and} \quad L_o^* = \frac{L_{bo}}{L_{bc}} \quad \text{Equation 43}$$

For turbulent flow, $n = 0.6$. The value of J_s will usually be between 0.85 and 1.0.

Shell Side Heat Transfer Coefficient

- 1) Calculate the shell side mass velocity (G_s), Reynolds Number (Re_s) and Prandtl Number (Pr_s):

$$G_s = \frac{M_s}{S_m} \quad \text{Equation 44}$$

$$Re_s = \frac{dG_s}{\mu} \quad \text{and} \quad Pr_s = \frac{\mu_s c_{ps}}{k_s} \quad \text{Equation 45}$$

- 2) Calculate the ideal heat transfer coefficient (h_i) given by

$$h_{id} = \frac{j_i c_{ps} G_s (\phi_s)^n}{Pr_s^{\frac{2}{3}}} \quad \text{Equation 46}$$

The term j_i is the ideal Colburn j factor for the shell side and can be determined from the appropriate Bell-Delaware curve for the tube layout and pitch and a typical curve.

$$j_i = 1.73Re_s^{(-0.694)} \quad \text{for } 1 \leq Re_s < 100 \quad \text{Equation 47 (a)}$$

$$= 0.717Re_s^{(-0.574)} \quad \text{for } 100 \leq Re_s < 1000 \quad \text{Equation 47 (b)}$$

$$\equiv 0.236Re_s^{(-0.346)} \quad \text{for } 1000 \leq Re_s \quad \text{Equation 47 (c)}$$

The term $(\phi_s)^n$ is the viscosity correction factor, which accounts for the viscosity gradient at the tube wall versus the viscosity at the bulk mean temperature of the fluid and is given by

$$(\phi_s)^n = \left(\frac{\mu_s}{\mu_w}\right)^{0.14} \quad \text{Equation 48}$$

For liquids, ϕ_s is greater than 1 if the shell side fluid is heated, and less than 1 when shell side fluid is cooled. In order to determine μ_w , it is essential to determine T_w , which is estimated as follows using the approximate values of h_o and h_i :

$$T_w = T_{t,av} + \frac{T_{s,av} - T_{t,av}}{1 + h_i h_o} \quad \text{Equation 49}$$

where $T_{s,av}$ and $T_{t,av}$ denote the average mean metal temperatures of shell and tube, both of them being the arithmetic means of inlet and outlet fluid temperatures on the shell side and tube side respectively.

3) Calculate the shell side heat transfer coefficient given by

$$h_o = h_{ia} J_c J_s J_b J_r \quad \text{Equation 50}$$

Tube Side Heat Transfer Coefficient

- 1) Calculate the tube side mass velocity (G_t), Reynolds Number (Re_t), and Prandtl Number (Pr_t).

$$G_t = \frac{M_t}{A_t} \quad \text{for single pass} \quad \text{Equation 51(a)}$$

$$= \frac{M_t}{A_t/N_p} \quad \text{for } N_p \text{ passes} \quad \text{Equation 51 (b)}$$

$$\text{where } A_t = \frac{\pi}{4} d_t^2 N_t$$

and where A_t is the tube side flow area, N_p the number of tube side passes, N_t the number of tubes and

$$Re_t = \frac{G_t d_t}{\mu_t} \quad \text{and} \quad Pr_t = \frac{\mu_t c_{pt}}{k_t} \quad \text{Equation 52}$$

- 2) Calculate the tube side heat transfer, h_i : Sieder-Tate Equation

$$\frac{h_i d_t}{k_t} = 0.027 Re_t^{0.8} Pr_t^{0.33} \left(\frac{\mu_t}{\mu_w} \right)^{0.14} \quad \text{Equation 53}$$

After determining the overall heat transfer coefficient, the next step in this project is to determine the overall heat transfer coefficient based on the daily plant operation data. This can be done by using the daily data from the plant and from there, proceed to determine the daily fouling resistance by calculating the value of

$\frac{1}{U_{actual}} - \frac{1}{U_{clean}}$. Ebert and Panchal model is based on the analysis of the high temperature furnace tube-side coking data reported by Scarborough *et al.* Due to the different in origin of the crude oil, the parameters have to be determined in the model as different crude oil has different components and impurities in it.

The Ebert-Panchal model (Equation 4) can be applied in this project as for the heat exchanger, the fouling condition on the heat exchanger is found to be more severe on the tube side. The parameters were determined by using Excel's solver function in order to get a calculated fouling rate curve that fits the actual fouling curve obtained from the plant data. Once the parameters for the Ebert-Panchal model (Equation 4) have been determined, the operating conditions that lead to non fouling condition or the near zero fouling rate can be determined. Ebert-Panchal model has been selected as the study approach in this project as it is the basic model of the fouling threshold model and other fouling threshold models are the modifications to the Ebert-Panchal model due to the difference in the origin of crude oil.

The milestones of the project included in a Gantt chart which is as shown in Figure 2. The key milestones for this whole final year project have been divided into several parts as follows:

- i. Submission of selected topic
- ii. Submission of preliminary report
- iii. Submission of Progress Report 1
- iv. Attend seminar evaluated by internal examiner
- v. Submission of interim report
- vi. Oral Presentation 1

- vii. Submission of Progress Report 2
- viii. Submission of Progress Report 3
- ix. Attend Seminar 2
- x. Poster exhibition
- xi. Submission of dissertation (soft bound)
- xii. Oral Presentation 2
- xiii. Submission of dissertation (hard bound)

The tool that is needed to complete this project includes software such as PetroSim, Microsoft Excel and Matlab.

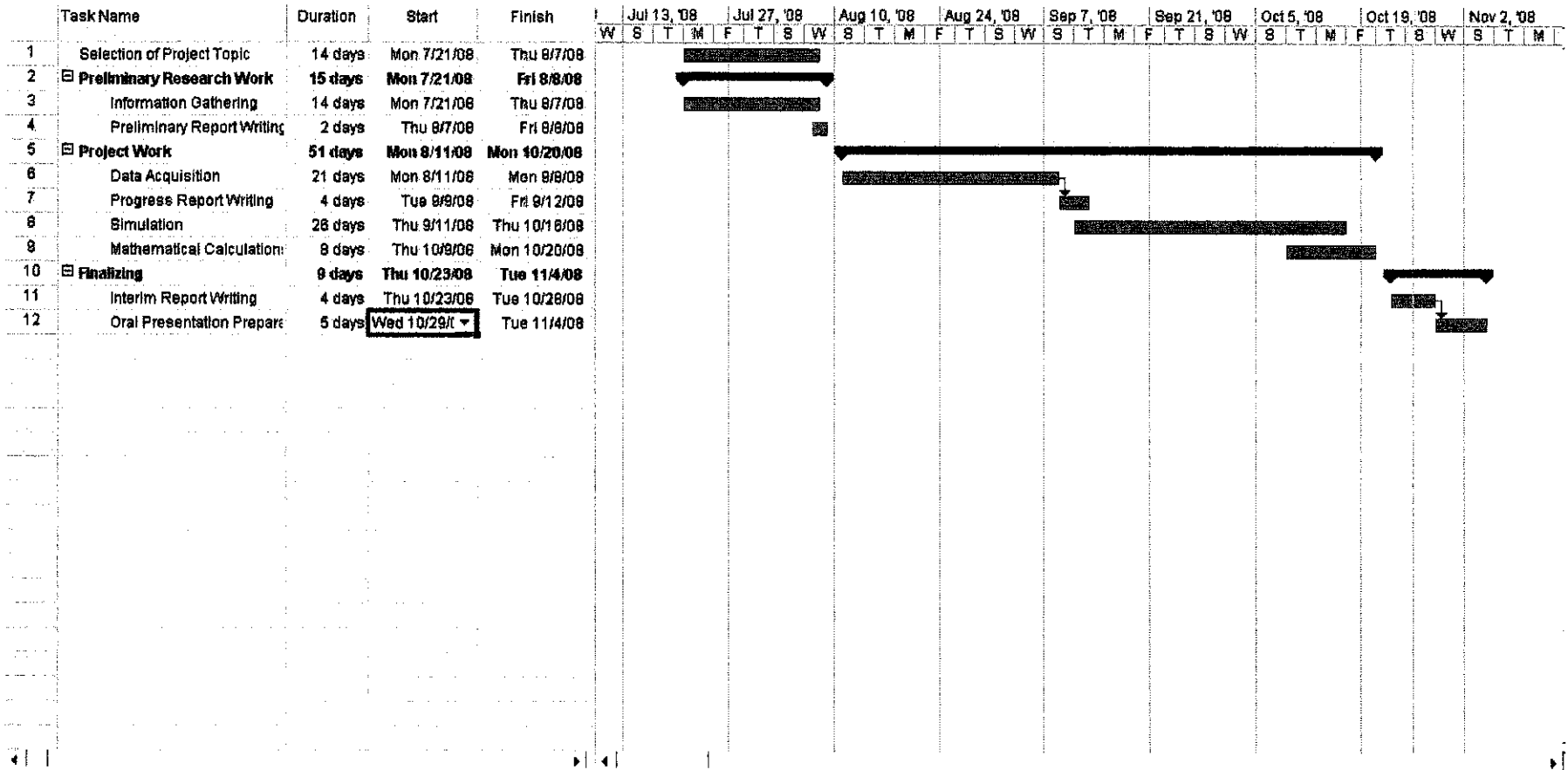


Figure 3: Gantt chart for the Final Year Project - Semester 1

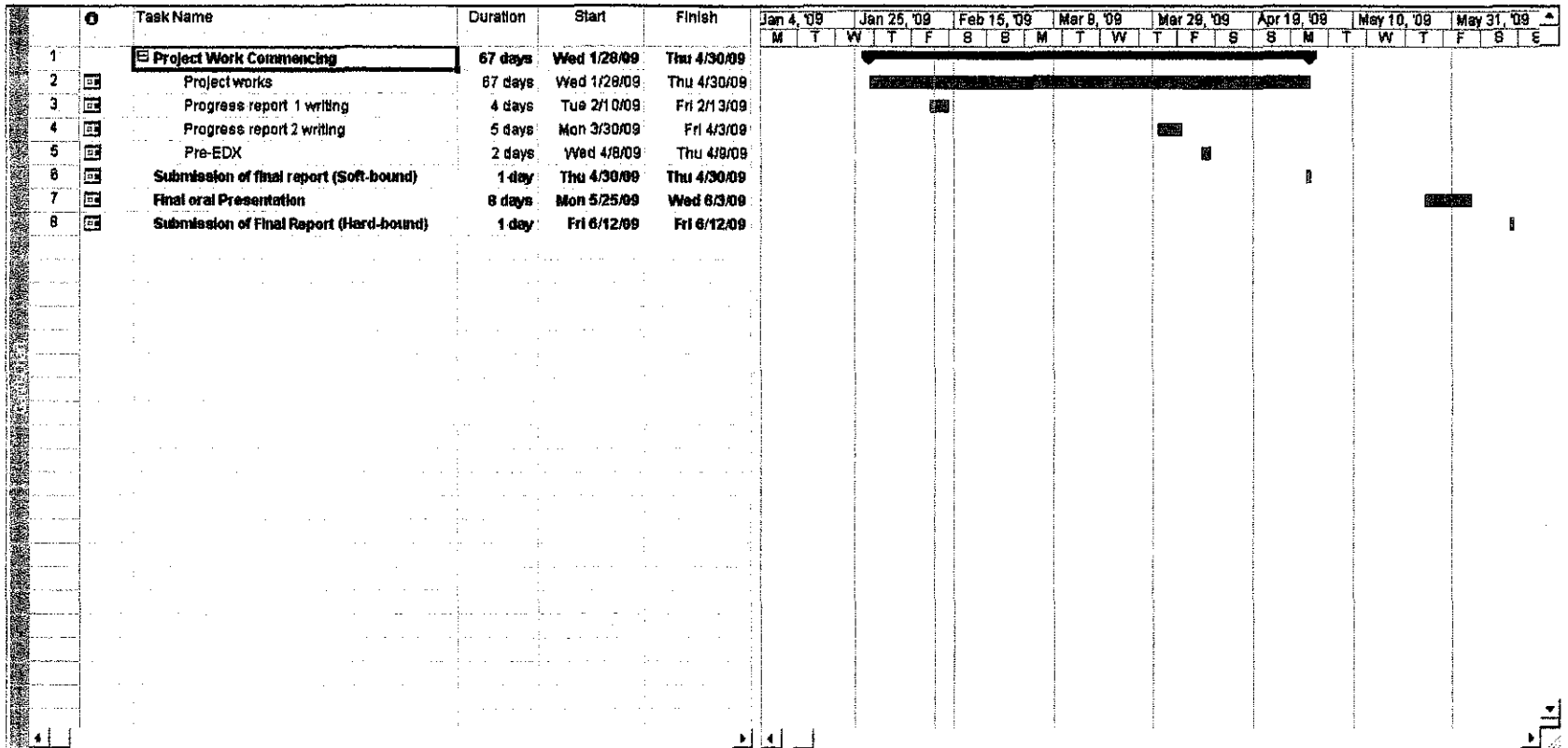


Figure 4: Gantt chart for the Final Year Project - Semester 2

CHAPTER 4

RESULTS AND DISCUSSION

Table 1: Percentage error comparison between conventional and Bell-Delaware methods

Heat Transfer Properties	Percentage Error (%)	
	Conventional	Bell-Delaware
Shell-side film coefficient, H_o (W/m ² K)	137.98	32.70
Tube-side film coefficient, H_i (W/m ² K)	63.87	50.16
Average	100.93	41.43

From Table 1, the average percentages of error for Bell-Delaware and conventional methods are 41.43 and 100.93 respectively. As the Bell-Delaware method gives a more precise computational outcome, this method was used in subsequent calculations.

Table 2: Data on heat exchanger for clean condition

	Heat exchanger
Shell-side film coefficient, H_o (W/m ² K)	753.7875
Tube-side film coefficient, H_i (W/m ² K)	836.5051
Overall Heat Transfer Coefficient, U (W/m ² K)	344.06
Heat Transfer Rate, Q (W)	4.3907 X 10 ⁶

For a heat exchanger in clean condition, the fouling resistance on both side, R_{fo} and R_{fi} can be dropped off from Equation 3 resulting the overall heat transfer coefficient,

$$U \text{ is redefined as } U = \frac{1}{\left(\frac{1}{h_o}\right) + \left(\frac{l}{k_m \times Am}\right) + \left(\frac{1}{h_i \times A_i}\right)}$$

Using the value of U at clean condition, the heat transfer rate, Q can be determined by Equation 2. From the parameters tabulated in Table 2, the heat transfer rate, Q for the heat exchanger at clean condition therefore will be 4.391 MW.

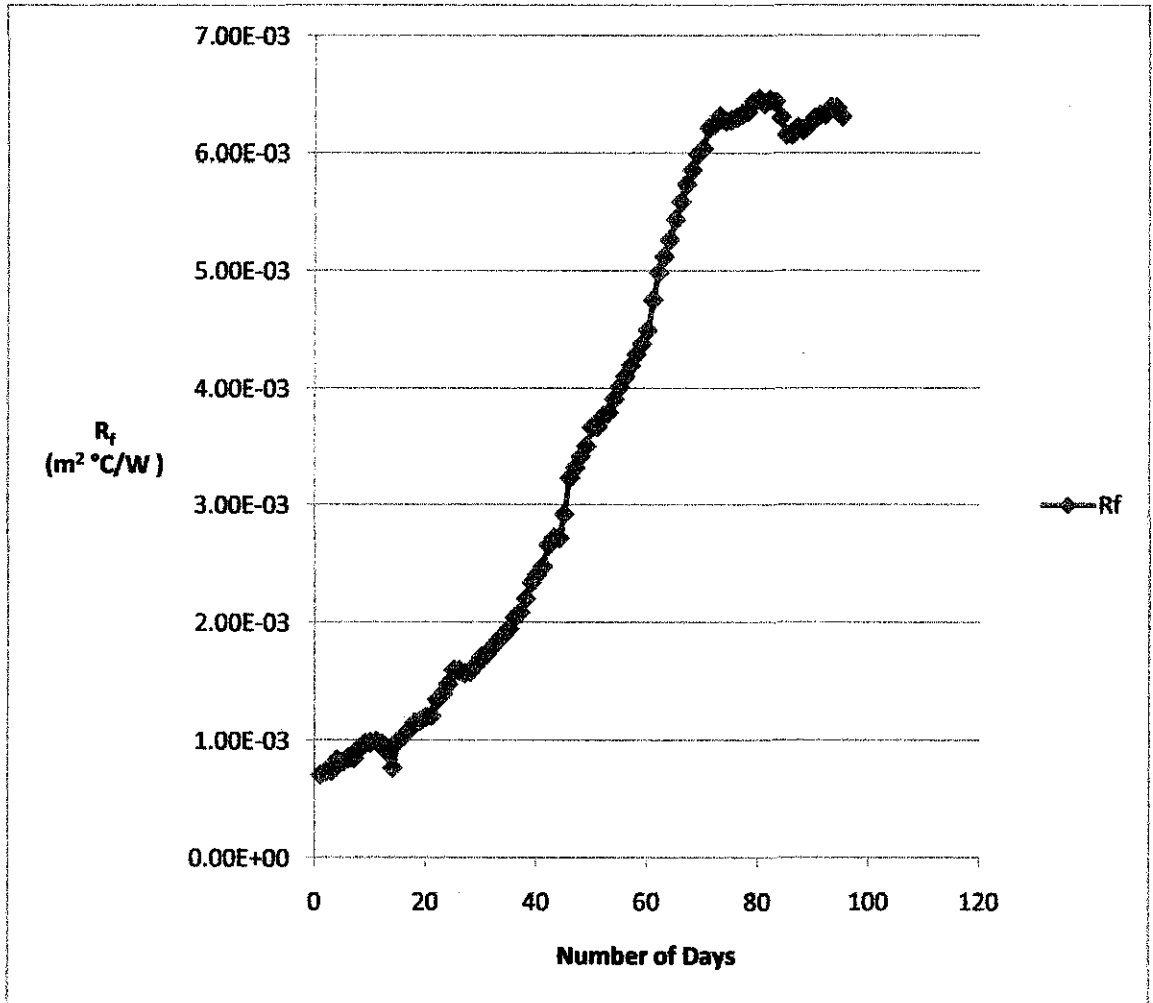


Figure 5: Graph of fouling resistance, R_f ($\text{m}^2 \text{ }^\circ\text{C/W}$) vs time (Number of Days).

Figure 5 shows that the fouling resistance given by the foulant found in the heat exchanger after running the heat exchanger for 95 days. As it has been shown, heat exchanger would experience asymptotic fouling when the fouling resistance, R_f increases daily till a point where the fouling resistance is maximum and the fouling curve flattens out. At this point the rate of foulant deposition is the same as the rate of foulant removal.

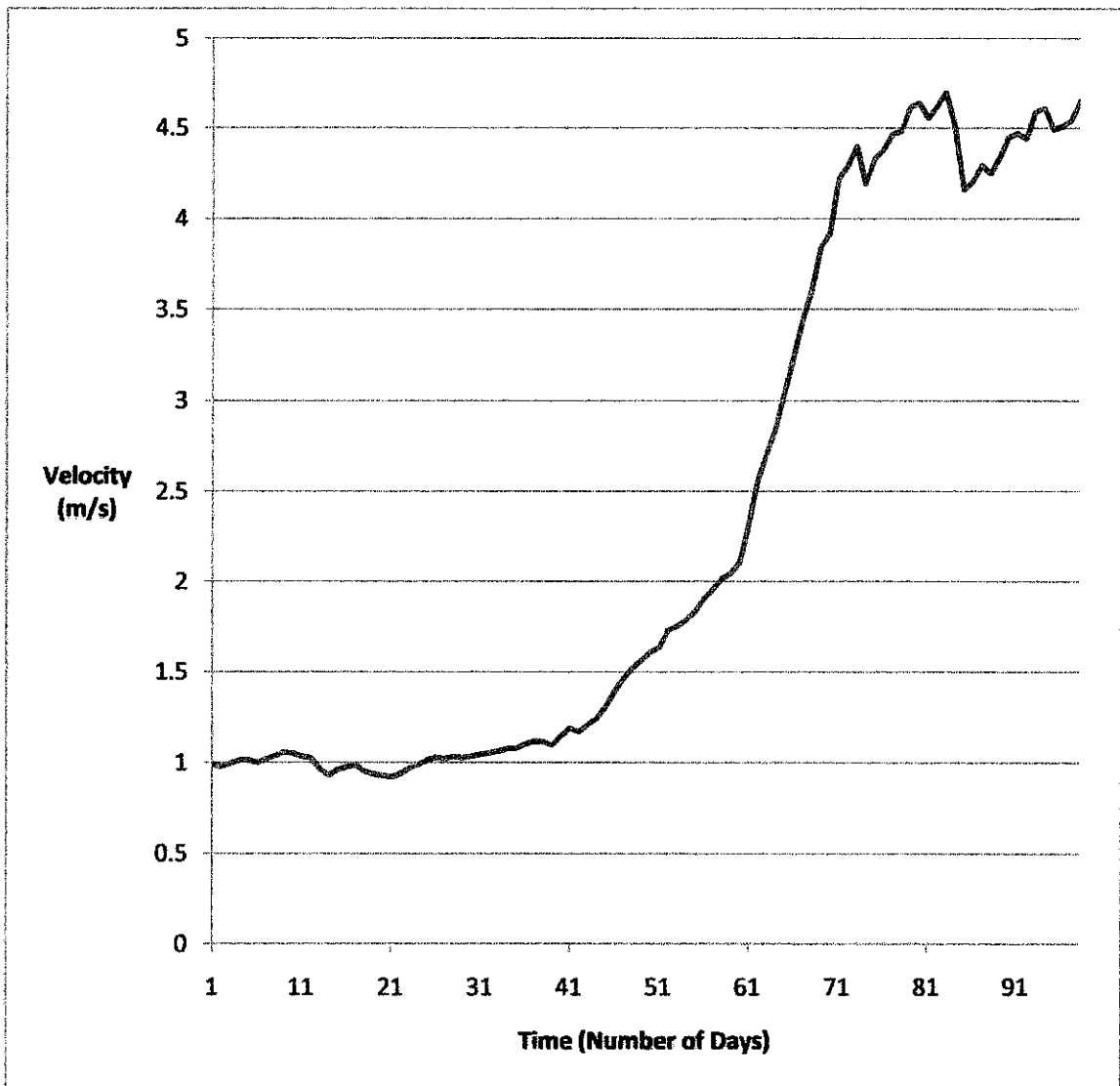


Figure 6: Graph of velocity (m/s) vs time (Number of Days)

As the size of the foulant gets thicker daily, the flow area in the tube becomes smaller and the fluid flow velocity increases as fluid velocity is inversely proportional to the fluid flow area. Figure 6 shows the fluid flow velocity in the tube side for the heat exchanger for the first 95 days. The velocity from day 41 starts to accelerate as the fouling rate has increased exponentially starting from day 40 (which can be observed from Figure 5) and the flow area in the tube decreases which lead to increases in fluid velocity with the volumetric flow rate remains unchanged.

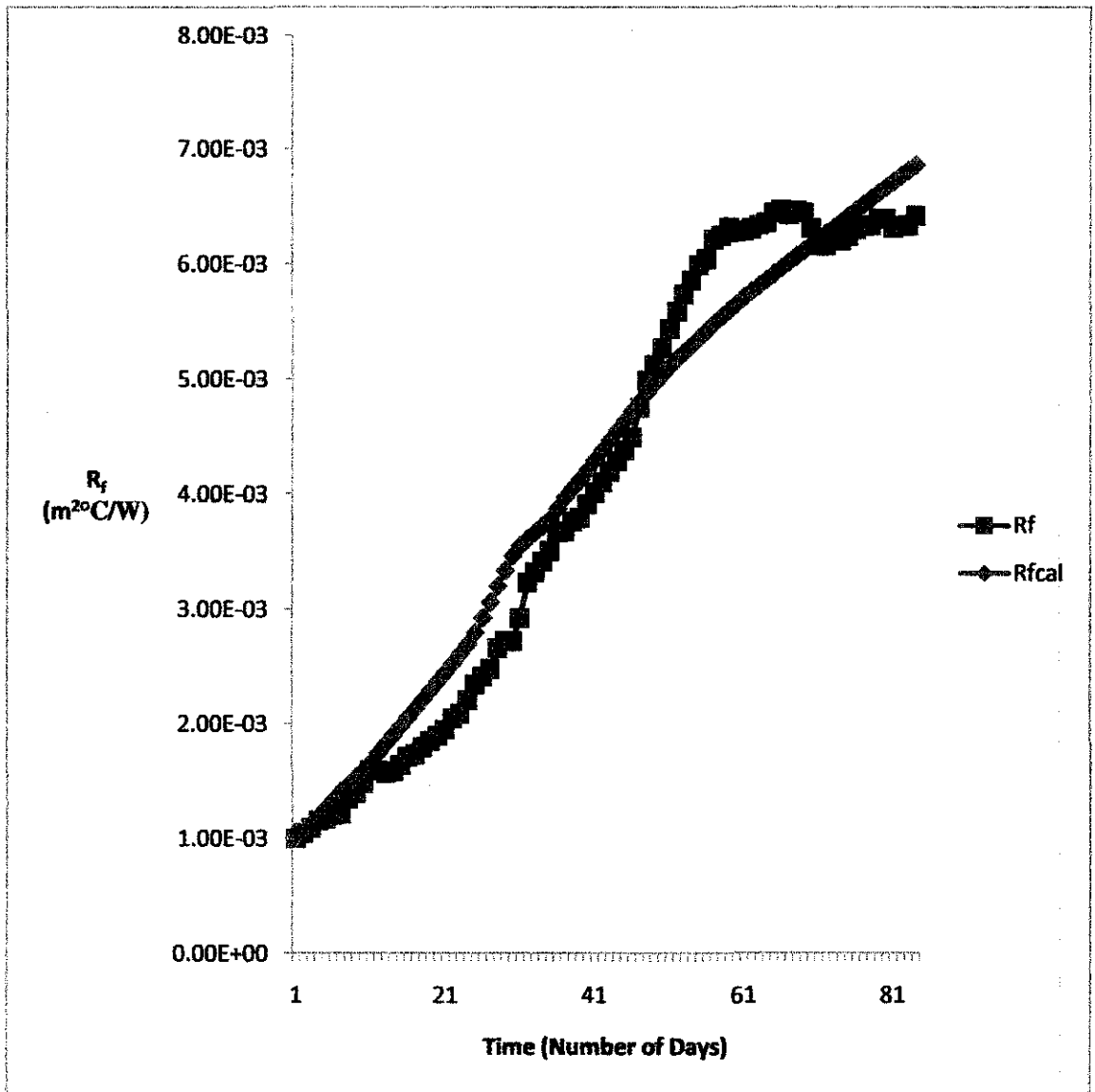


Figure 7: Graph of fouling resistance, R_f ($m^2°C/W$) vs time (Number of Days)

Figure 7 shows the two curves of the calculated fouling resistance and the actual fouling resistance. The calculated fouling resistance was calculated by using the Ebert-Panchal model (Equation 4) where the parameters of the model had been found to be $A_1 = 520074.782786046 \text{ K m}^2/\text{kWh}$, $B = 0.88$, $E_1 = 44.638 \text{ kJ/mol}$, $C_1 = 6 \times 10^{-8} \text{ m}^2 \cdot \text{Km}^2/\text{kW} \cdot \text{Pa} \cdot \text{h}$. The average absolute relative error percentage found by using this set of parameters is about 10.17 % and its sum of errors squared is 1.28×10^{-5} .

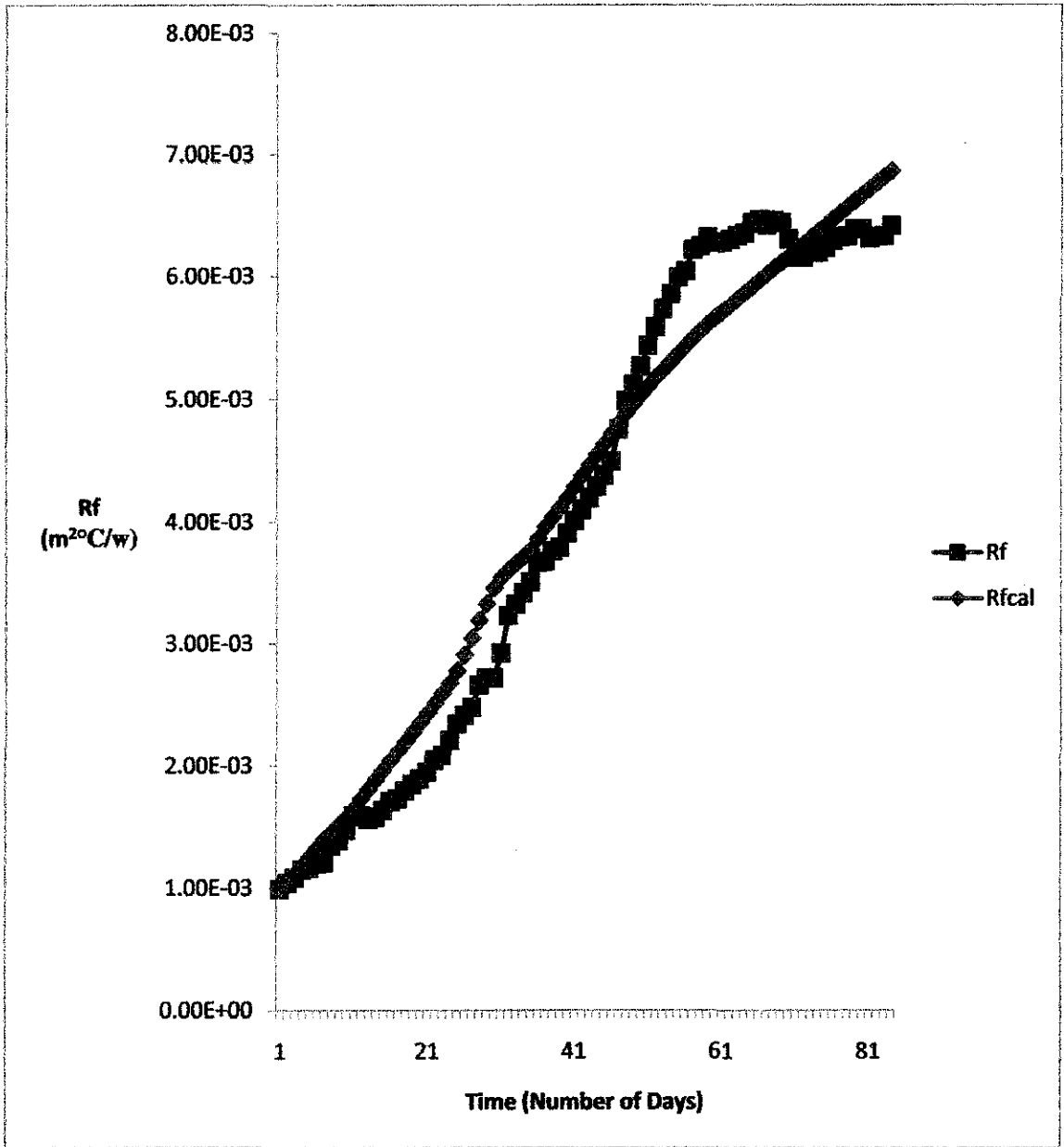


Figure 8: Graph of fouling resistance, R_f ($m^2°C/W$) vs time (Number of Days)

Figure 8 shows the two fouling curves of the calculated fouling resistance and the actual fouling resistance, with a different set of parameters for the Ebert-Panchal model where $A_1 = 1092288.21424247 \text{ K m}^2/\text{kWh}$, $B = 0.88$, $E_1 = 46.999 \text{ kJ/mol}$, $C_1 = 5.93 \times 10^{-8} \text{ m}^2 \cdot \text{Km}^2/\text{kW.Pa.h}$. The average absolute relative error percentage found by using this set of parameters is about 9.94 % and its sum of errors squared is 1.25×10^{-5} .

Therefore the parameters set of $A_1 = 1092288.21424247 \text{ K m}^2/\text{kWh}$, $B = 0.88$, $E_1 = 46.999 \text{ kJ/mol}$, $C_1 = 5.93 \times 10^{-8} \text{ m}^2 \cdot \text{Km}^2/\text{kW.Pa.h}$ will be used in this project as it gives us a smaller absolute error percentage and sum of squared errors.

CHAPTER 5

CONCLUSION AND RECOMMENDATIONS

Bell-Delaware method provides more accurate values compared to the data sheet given rather than the conventional method. Therefore Bell-Delaware method is used in determining the heat exchanger design properties.

The parameters of the Ebert and Panchal fouling threshold model were successfully determined based on industrial data. The simulated fouling curve follows closely with the actual fouling curve from industrial data.

For the future work, the operating threshold fluid flow velocity for the tube side can be determined from the parameters of the Ebert-Panchal model. The operating threshold fluid flow velocity will result in near zero fouling rate for the heat exchanger.

REFERENCES

- 1) Srinivasan, M. and Watkinson, A.P. 2004, "Fouling of Some Canadian Crude Oils", *2003 ECI Conference on Heat Exchanger Fouling and Cleaning: Fundamentals and Applications*, Santa Fe, New Mexico, USA.
- 2) Shinji Isogai and Mitsutaka Nakamura, 2004, "Analysis and Steps to Mitigate Heat Exchanger Fouling in an Aromatics Plant", *2003 ECI Conference on Heat Exchanger Fouling and Cleaning: Fundamentals and Applications*, Santa Fe, New Mexico, USA.
- 3) Polley, G.T., Wilson, D.I., Yeap, B.L., and Pugh, S.J. 2002. *Evaluation of laboratory crude oil threshold fouling data for application to refinery pre-heat trains*. Elsevier Science Ltd.
- 4) Bories, M. and Patureaux, T. 2004, "Preheat Train Crude Distillation Fouling Propensity Evaluation by the Ebert and Panchal Model", *2003 ECI Conference on Heat Exchanger Fouling and Cleaning: Fundamentals and Applications*, Santa Fe, New Mexico, USA.
- 5) Wilson, D.I., Polley, G.T. and Pugh, S.J. 2005, "Ten Years of Ebert, Panchal and the 'Threshold Fouling' Concept", *ECI Symposium Series, Volume P2: Proceedings of 6th International Conference on Heat Exchanger Fouling and Cleaning*, Engineering Conferences International, Kloster Irsee, Germany, June 5-10, 2005
- 6) Mohammad Reza Jafari Nasr and Mehdi Majidi Givi, 2005. *Modeling of crude oil fouling in preheat exchangers of refinery distillation units*. National Petrochemical Research and Technology Company, Islamic Republic of Iran.

- 7) Schreier, P.J.R. and Fryer, P.J. 1994. *Heat exchanger fouling: A model study of the scaleup of laboratory data*. Elsevier Science Ltd.
- 8) Nesta, J. and Bennett, C.A. 2005, "Fouling Mitigation By Design", *ECI Symposium Series, Volume P2: Proceedings of 6th International Conference on Heat Exchanger Fouling and Cleaning*, Engineering Conferences International, Kloster Irsee, Germany, June 5-10, 2005
- 9) Kuppan, T. 2000, *Heat Exchanger Design Handbook*, New York, Marcel Dekker.
- 10) Saleh, Z.S., Sheikholeslami, R. and Watkinson, A.P. 2005, "Bleeding Effects On Fouling of Four Crude Oils", *ECI Symposium Series, Volume P2: Proceedings of 6th International Conference on Heat Exchanger Fouling and Cleaning*, Engineering Conferences International, Kloster Irsee, Germany, June 5-10, 2005
- 11) Yeap, B.L., Wilson, D.I., Polley, G.T. and Pugh, S.J. 2004, "Retrofitting Crude Oil Refinery Heat Exchanger Networks to Minimize Fouling While Maximizing Heat Recovery", *2003 ECI Conference on Heat Exchanger Fouling and Cleaning: Fundamentals and Applications*, Santa Fe, New Mexico, USA.
- 12) Yeap, B.L., Wilson, D.I., Polley, G.T. and Pugh, S.J. 2003, "Mitigation of crude oil refinery heat exchanger fouling through retrofits based on thermo-hydraulic models", *Chemical Engineering Research and Design*
- 13) Epstein, Norman 1988, "General Thermal Fouling Models" in L.F. Melo, T.R. Bott and C.A. Bernardo *Fouling Science and Technology*, Netherlands, Kluwer Academic Publishers.

- 14) Ebert. W and Panchal, C.B., 1995, "Analysis of Exxon crude-oil, slip stream coking data" , *Engineering Foundation Conference on Fouling Mitigation of Heat Exchangers*, California, USA

- 15) BOS-HATTEN, Inc. <<http://www.bos-hatten.com/temadia.html> >, 4 June 2009

- 16) Donald Q. Kern, *Process Heat Transfer: International Edition 1965*, McGraw-Hill Book Company, Inc.

- 17) Watkinson A.P. and Wilson D.I., 1997, "Chemical Reaction Fouling: A Review", *Experimental Thermal and Fluid Science 1997*, Elsevier Science Inc.

APPENDIX

Appendix 1-1: Crude Properties

Table 3: Crude properties for the simulation

CRUDE PROPERTIES	unit	A	B	C	D	E
Density @ 15°C	(kg/l)	0.8032	0.8636	0.694	0.7041	0.8011
Basic Sediment & Water	(vol. %)	0.35	0.026	0.05	0.05	0.05
Water	(vol. %)	0.275	0.025	0.05	0.05	0.1
Reid Vapor Pressure	(kPa)	51.7	29	89.9	78.13	
Total Acid Number	(mgKOH/g)	0.13	0.27	0.05	0.05	0.83
Flash Point	(°C)	25	19	25	25	0
Pour Point	(°C)	21	-9	-60	-60	3
Total Sulphur	(wt %)	0.028	0.078	0.015	0.0253	0.08
Salt Content	(lb/1000bbls)	28	10.1	20	20	0.009
Nitrogen Content	(ppm)	189	272	3	2	189
Ash Content	(wt %)	0.003	0.001	0.001	0.001	0.005
Wax Content	(wt %)	8	2.3	5	5	5.64
Kinematic Viscosity @ 70degC	(cSt)	1.45	1.788	1.519	0.448	1.559
Characterisation Factor		12	11.5	13.8	12.11	12.03
Gross Calorific Value	(MJ/kg)	47.12	44.35	47.3709	47.447	46.24
Mercury	(ppb)	10	2	2	7	
Asphaltenes	(wt %)	0.5	0.5	0.01	0.01	0.07
Sodium (Na)	ppm	8	3	1	1	9.06
Potassium (K)	ppm	< 1	0.2	< 1	< 1	1.09
Copper (Cu)	ppm	< 1	< 0.1	< 1	< 1	0.14
Lead (Pb)	ppm	< 1	< 0.1	< 1	< 1	0.82
Iron (Fe) PRSS	ppm	2.74	0.4	3.83	2.9	0.82
Nickel (Ni)	ppm	< 1	0.4	< 1	< 1	0.56
Vanadium (V)	ppm	< 1	< 0.1	< 1	< 1	6.08
Arsenic (As)	ppm	< 1	< 0.1	< 1	< 1	0

Asphaltene drop out	mg/l	4		2	2	
aromatic	wt%	21		9	16	
saturates (P+N)	wt%	77		91	91	
Iso-octane	mg/l	25		4	4	
Filterable solid	mg/l	25		4	4	